Preprints of the 21st IFAC World Congress (Virtual)
Berlin, Germany, July 12-17, 2020

Passivity-based variable impedance control for redundant manipulators

Youssef Michel * **Christian Ott** ** **Dongheui Lee** *,**

* *Human-centered Assistive Robotics, Technical University of Munich (TUM)*

** *Institute of Robotics and Mechatronics, German Aerospace Center (DLR)*

Abstract: Kinematic redundancy significantly improves the dexterity and flexibility of robotic manipulators. The redundant degrees of freedom can be exploited to fulfill additional tasks that can be executed without disturbing the primary task. In this work, we investigate how a time varying impedance behavior can be embedded into redundant manipulators where it is desired to achieve such a behavior both for the primary and null space tasks. A passivity based controller is developed, relying on the concept of energy tanks which are filled by the dissipated power in the system, and compensate for non-passive control actions. This guarantees that the system remains passive, which ensures stable interactions with any passive environment. The method is validated in simulations where the interactive behavior of the main and null space tasks is specified by a time varying stiffness profile.

Keywords: Robot control, Variable Impedance control, Redundant manipulators, Passivity-based control, Energy tanks

1. INTRODUCTION

A robot is said to be kinematically redundant if it possesses more degrees of freedom (DOF) than necessary to accomplish a desired task. This can be effectively exploited by the robot to enhance its flexibility and dexterity by assigning additional tasks that can be executed without disturbing the main one. Such redundancy has been used for improving manipulability by avoiding singularities (Yoshikawa, 1985), avoiding joint limits (Liegeois, 1977), or assigning a specific interactive behavior in the robot's null space (Ott et al., 2015).

In this regard, the field of interaction control has received special attention over the past decade. Most notably, the concept of impedance control introduced in the seminal work of Hogan (1984). Instead of controlling position or force explicitly, impedance control aims at controlling the dynamic relationship between them using a second order system consisting of a virtual mass, spring and damper.

Interestingly, humans use a similar strategy for controlling their interactive behavior (Tee et al., 2004). In addition, humans excel in their ability to interact with different environments by continuously modulating their end point force and impedance by the concurrent co-activation/contraction of suitable muscle pairs (Franklin et al., 2003). Inspired by that, variable impedance control methods have emerged aiming at endowing robots with such levels of adaptation. Variable impedance control strategies can be learned with techniques such as reinforcement learning as done in Buchli et al. (2010), and in Winter et al. (2016) to learn fully coupled stiffness behaviors. In both works, a user defined objective function is iteratively optimized resulting in a time varying stiffness profile. An adaptive biomimetic controller based on human motor control theory was derived in Yang et al. (2011) for reaching the optimal interactive behavior that minimizes instability and effort by adapting feedforward force and impedance. This controller was later extended in Ganesh et al. (2012) for contact tooling and haptic exploration. In Lee and Ott (2011), impedance control with variable stiffness is utilized for incremental kinesthetic teaching, ensuring tracking accuracy in free-motion, while allowing compliant behavior in case of interactions. Peternel et al. (2016) used impedance control with stiffness adaptation for a collaborative sawing task. Depending on the task stage, the robot alternates between being stiff and compliant delivering the required physical assistance for the human partner.

Surprisingly, however, robot redundancy has often been neglected in variable impedance control analysis. Ficuciello et al. (2015) considered that aspect when they proposed an approach for the state-dependent modulation of the robot end point damping and inertia during human-robot co-manipulation. The redundancy of the robot is exploited to decouple the end effector equivalent inertia, maximizing the region of stability in the impedance parameter space. A similar idea was proposed in Ott et al. (2011), where a passivity observer is used to monitor the interaction between the robot and the environment, and a null space controller injects additional dissipation in the system whenever the environment becomes active.

In this paper, building on the work of Ott et al. (2015), we present a passivity-based approach that takes into account the redundant degrees of freedom for the controller formulation, and aim at achieving an impedance behavior with a time varying stiffness both for the main and null space tasks. Unfortunately, stiffness variations in general are considered to be a non-passive action (Ferraguti et al., 2013; Kronander and Billard, 2016) and represent a source of activity in the system. The problem is further aggravated for redundant manipulators since the use of null space projections by itself is a reason for the loss of pas-

sivity in the system (Dietrich et al., 2016). As delineated in Stramigioli (2015), passivity is a must for robots in physical interaction, since it is a necessary requirement for a stable and safe interaction with arbitrary passive environments.

In this work, passivity in the system is guaranteed at all times thanks to the use of energy tanks. Since they were inititally proposed in Duindam and Stramigioli (2004), energy tanks were featured prominently in many robotic applications. They have been used for bilateral telemanipulation (Franken et al., 2011), variable stiffness control (Ferraguti et al., 2013), passification of null space projections (Dietrich et al., 2016, 2017) and force tracking control both for flexible joint manipulators (Schindlbeck and Haddadin, 2015) and hexarotors (Rashad et al., 2019).

The rest of this paper is organized as follows. Section 2 presents some preliminaries regarding the tasks definitions and the formulation of the hierarchical dynamics of the primary and null space tasks. Section 3 highlights the reasons for the loss of passivity in the system. Section 4 explains the proposed solution and the design of the energy tank for the preservation of passivity in the system, while section 5 presents the proof of passivity in the system. The validation of the presented approach in simulation is carried out in section 6 and finally, section 7 concludes the paper and provides directions for future work.

2. PRELIMINARIES

In this section, we briefly review some of the preliminary concepts related to prioritized tasks modeling and the hierarchical definition of tasks dynamics (Ott et al., 2008). The considered rigid body dynamics can be expressed as

$$\boldsymbol{M}(\boldsymbol{q})\ddot{\boldsymbol{q}} + \boldsymbol{C}(\boldsymbol{q},\dot{\boldsymbol{q}})\dot{\boldsymbol{q}} + \boldsymbol{g}(\boldsymbol{q}) = \boldsymbol{\tau} + \boldsymbol{\tau}_{\text{ext}}\,, \tag{1}$$

where $\boldsymbol{q} \in \mathbb{R}^n$ are the generalized coordinates, $\boldsymbol{M}(\boldsymbol{q}) \in \mathbb{R}^{n\times n}$ is the symmetric, positive definite inertia matrix. $\boldsymbol{C}(\boldsymbol{q},\dot{\boldsymbol{q}}) \in \mathbb{R}^{n\times n}$ is the Coriolis and centrifugal matrix, and satisfies $\dot{\boldsymbol{M}}(\boldsymbol{q}) = \boldsymbol{C}(\boldsymbol{q},\dot{\boldsymbol{q}}) + \boldsymbol{C}^T(\boldsymbol{q},\dot{\boldsymbol{q}})$. The gravity torque is given by $\boldsymbol{g}(\boldsymbol{q}) \in \mathbb{R}^n$, the control input and the external torques are denoted by $\boldsymbol{\tau} \in \mathbb{R}^n$ and $\boldsymbol{\tau}_{\text{ext}} \in \mathbb{R}^n$, respectively. In the following, we consider a task hierarchy consisting of two priority levels with a primary task $\boldsymbol{x}_1$ and a null space task $\boldsymbol{x}_2$, which shall be executed as good as possible without disturbing the main task. The tasks are given by $\boldsymbol{x}_i = \boldsymbol{f}_i(\boldsymbol{q})$, where $\boldsymbol{f}_i(\boldsymbol{q})$ is the nonlinear forward kinematic map for $i = 1, 2$. On a differential level, the tasks are defined by:

$$\dot{\boldsymbol{x}}_1 = \boldsymbol{J}_1(\boldsymbol{q})\dot{\boldsymbol{q}}\ ,\ \ \boldsymbol{J}_1(\boldsymbol{q}) = \frac{\partial \boldsymbol{f}_1}{\partial \boldsymbol{q}} \tag{2}$$

$$\dot{\boldsymbol{x}}_2 = \boldsymbol{J}_2(\boldsymbol{q})\dot{\boldsymbol{q}}\ ,\ \ \boldsymbol{J}_2(\boldsymbol{q}) = \frac{\partial \boldsymbol{f}_2}{\partial \boldsymbol{q}} \tag{3}$$

where $\boldsymbol{J}_1 \in \mathbb{R}^{m_1\times n}$ and $\boldsymbol{J}_2 \in \mathbb{R}^{m_2\times n}$ are the corresponding task Jacobians relating joint-space velocities to task-space velocities. However, since the task space velocities $\dot{\boldsymbol{x}}_1$, $\dot{\boldsymbol{x}}_2$ feature couplings between the two priority levels, we consider the following coordinate transformation (Park et al., 1999)

$$\dot{\boldsymbol{q}} = [\boldsymbol{J}_1(\boldsymbol{q})^{\boldsymbol{W}+}\ \ \boldsymbol{Z}(\boldsymbol{q})^T] \begin{bmatrix}\dot{\boldsymbol{x}}_1 \\ \boldsymbol{v}_n\end{bmatrix}\,, \tag{4}$$

where $\boldsymbol{J}_1(\boldsymbol{q})^{\boldsymbol{W}+}$ is the weighted pseudo inverse of $\boldsymbol{J}_1(\boldsymbol{q})$ with a weight $\boldsymbol{W}(\boldsymbol{q})$ [1], $\boldsymbol{Z}(\boldsymbol{q}) \in \mathbb{R}^{(n-m_1)\times n}$ is a full row rank null space base matrix of $\boldsymbol{J}_1(\boldsymbol{q})$ and can be found via singular value decomposition of $\boldsymbol{J}_1(\boldsymbol{q})$. The minimal parameterization of the weighted self motion velocity $\boldsymbol{v}_n \in \mathbb{R}^{m_2\times n}$ is given by

$$\boldsymbol{v}_n = \boldsymbol{N}(\boldsymbol{q})\dot{\boldsymbol{q}}\,, \tag{5}$$

with $\boldsymbol{N}(\boldsymbol{q}) = (\boldsymbol{Z}\boldsymbol{W}\boldsymbol{Z}^T)^{-1}\boldsymbol{Z}\boldsymbol{W}$ [2]. We can now define the extended jacobian of the system as

$$\boldsymbol{J}_e(\boldsymbol{q}) = \begin{bmatrix}\boldsymbol{J}_1(\boldsymbol{q}) \\ \boldsymbol{N}(\boldsymbol{q})\end{bmatrix}\ ,\ \boldsymbol{J}_e(\boldsymbol{q})^{-1} = \begin{bmatrix}\boldsymbol{J}_1^{\boldsymbol{W}+}(\boldsymbol{q}) \\ \boldsymbol{Z}(\boldsymbol{q})^T\end{bmatrix} \tag{6}$$

and the extended space velocities

$$\dot{\boldsymbol{x}}_e = \begin{bmatrix}\dot{\boldsymbol{x}}_1 \\ \boldsymbol{v}_n\end{bmatrix} = \boldsymbol{J}_e\dot{\boldsymbol{q}}\,, \tag{7}$$

which are kinematically decoupled in the sense that $\boldsymbol{J}_1\boldsymbol{Z}^T\boldsymbol{v}_n = \boldsymbol{0}$ and $\boldsymbol{N}\boldsymbol{J}_1^{\boldsymbol{W}+}\dot{\boldsymbol{x}}_1 = \boldsymbol{0}$. Assigning $\boldsymbol{W}(\boldsymbol{q}) = \boldsymbol{M}(\boldsymbol{q})$ and projecting the dynamics (1) into extended velocity space yields the dynamically consistent formulation of the hierarchical dynamics (Ott et al., 2008)

$$\boldsymbol{\Lambda}_e(\boldsymbol{q})\ddot{\boldsymbol{x}}_e + \boldsymbol{\mu}_e(\boldsymbol{q},\dot{\boldsymbol{q}})\dot{\boldsymbol{x}}_e = \boldsymbol{J}_e(\boldsymbol{q})^{-T}(-\boldsymbol{g}(\boldsymbol{q}) + \boldsymbol{\tau} + \boldsymbol{\tau}_{ext})\,, \tag{8}$$

where

$$\boldsymbol{\Lambda}_e = \boldsymbol{J}_e^{-T}\boldsymbol{M}\boldsymbol{J}_e^{-1} = \begin{bmatrix}\boldsymbol{\Lambda}_x(\boldsymbol{q}) & \boldsymbol{0} \\ \boldsymbol{0} & \boldsymbol{\Lambda}_n(\boldsymbol{q})\end{bmatrix}\,, \tag{9}$$

is the extended space inertia which is block diagonal thanks to the particular choice $\boldsymbol{W}(\boldsymbol{q}) = \boldsymbol{M}(\boldsymbol{q})$, which implies that no kinetic energy couplings exist between the priority levels. The extended space Coriolis and centrifugal matrix $\boldsymbol{\mu}_e$ is given by

$$\boldsymbol{\mu}_e = \boldsymbol{\Lambda}_e(\boldsymbol{J}_e\boldsymbol{M}^{-1}\boldsymbol{C} - \dot{\boldsymbol{J}}_e)\boldsymbol{J}_e^{-1} = \begin{bmatrix}\boldsymbol{\mu}_x(\boldsymbol{q},\dot{\boldsymbol{q}}) & \boldsymbol{\mu}_{xn}(\boldsymbol{q},\dot{\boldsymbol{q}}) \\ \boldsymbol{\mu}_{nx}(\boldsymbol{q},\dot{\boldsymbol{q}}) & \boldsymbol{\mu}_n(\boldsymbol{q},\dot{\boldsymbol{q}})\end{bmatrix}\,. \tag{10}$$

We can now define the control torque $\boldsymbol{\tau}$ as

$$\boldsymbol{\tau} = \boldsymbol{\tau}_g + \boldsymbol{\tau}_d + \boldsymbol{\tau}_1 + \boldsymbol{\tau}_2\,, \tag{11}$$

where $\boldsymbol{\tau}_g = \boldsymbol{g}(\boldsymbol{q})$ is a gravity compensation term. The control $\boldsymbol{\tau}_d = \boldsymbol{J}_1^T\boldsymbol{\mu}_{xn}\boldsymbol{v}_n + \boldsymbol{N}^T\boldsymbol{\mu}_{nx}\dot{\boldsymbol{x}}_1$ is a passive feedback with power $P_d = \boldsymbol{\tau}_d^T\dot{\boldsymbol{q}} = 0$ since $\boldsymbol{\mu}_{nx} = -\boldsymbol{\mu}_{xn}^T$, and has the role of removing the cross coupling Coriolis and centrifugal terms. The torques $\boldsymbol{\tau}_1$ and $\boldsymbol{\tau}_2$ will be designed to perform the control objective of the primary and null space tasks, respectively. We can now write the extended space dynamics as

$$\begin{aligned}\begin{bmatrix}\boldsymbol{\Lambda}_x & \boldsymbol{0} \\ \boldsymbol{0} & \boldsymbol{\Lambda}_n\end{bmatrix}\begin{bmatrix}\ddot{\boldsymbol{x}}_1 \\ \dot{\boldsymbol{v}}_n\end{bmatrix} + \begin{bmatrix}\boldsymbol{\mu}_x & \boldsymbol{0} \\ \boldsymbol{0} & \boldsymbol{\mu}_n\end{bmatrix}\begin{bmatrix}\dot{\boldsymbol{x}}_1 \\ \boldsymbol{v}_n\end{bmatrix} \\ = \boldsymbol{J}_e^{-T}(\underbrace{\boldsymbol{\tau}_1 + \boldsymbol{\tau}_2}_{\boldsymbol{\tau}_c} + \boldsymbol{\tau}_{ext})\,,\end{aligned} \tag{12}$$

with the skew symmetry of $(\dot{\boldsymbol{\Lambda}}_x - 2\boldsymbol{\mu}_x)$ and $(\dot{\boldsymbol{\Lambda}}_n - 2\boldsymbol{\mu}_n)$.

3. PROBLEM FORMULATION

As proven in Stramigioli (2015), having a stable interaction with any passive, possibly unknown environment requires the controlled robot to be ensured passive seen from the environment side. Within the control as interconnection paradigm, the plant and the controllers are no longer considered as signal processors, but rather energy exchanging systems that interact together through their corresponding power ports, with the controller regarded as another dynamical system interconnected to the plant in a power preserving manner (Secchi et al., 2007). Therefore, and relying

[1] $\boldsymbol{J}_1^{\boldsymbol{W}+} = \boldsymbol{W}^{-1}\boldsymbol{J}^T(\boldsymbol{J}\boldsymbol{W}^{-1}\boldsymbol{J}^T)^{-1}$

[2] For the sake of clarity, we omit dependency on $\boldsymbol{q}$ where obvious.

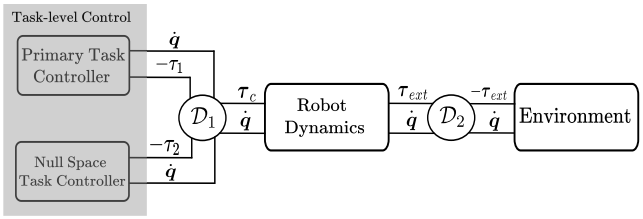

Fig. 1. Port-Based modeling of the system as an interconnection of the controllers, the robot dynamics (the plant) and the environment

on the fact that the interconnection of passive subsystems yields a passive system, we analyze the passivity of each subsystem independently with respect to its corresponding power port. As shown in Figure 1, the robot dynamics (12) is interconnected through the power port $(\boldsymbol{\tau}_{ext}, \dot{\boldsymbol{q}})$ which models the physical interaction with the environment. On the other hand, the port $(\boldsymbol{\tau}_c, \dot{\boldsymbol{q}})$ models the power exchange between the robot and the primary and null space tasks controllers, with the energy injected through this port is used for achieving the control objectives. The topology of the interconnections is defined by the power preserving *Dirac structures* $\mathcal{D}_1$ and $\mathcal{D}_2$ which represent a feedback interconnection.

3.1 Subsystem Passivity

Robot Dynamics The passivity of the extended task space dynamics (12) can be easily shown with the storage function

$$S_r = \frac{1}{2}\dot{\boldsymbol{x}}_e^T \boldsymbol{\Lambda}_e \dot{\boldsymbol{x}}_e \,, \tag{13}$$

which represents the sum of kinetic energies of the main and null space tasks. The time derivative of S_r along (12) is given by

$$\dot{S}_r = \dot{\boldsymbol{x}}_e^T \boldsymbol{J}_e^{-T}(\boldsymbol{\tau}_c + \boldsymbol{\tau}_{ext}) = \dot{\boldsymbol{q}}^T(\boldsymbol{\tau}_c + \boldsymbol{\tau}_{ext}) \,, \tag{14}$$

which shows passivity of the robot dynamics with respect to the pair $(\boldsymbol{\tau}_c + \boldsymbol{\tau}_{ext}, \dot{\boldsymbol{q}})$.

Primary task controller The goal of the primary task is to achieve a specific compliance around a virtual equilibrium $\boldsymbol{x}_{1,d}$. Compliance control is a special case of impedance control where inertia shaping and hence the feedback of external forces are avoided. The compliance behavior is defined by a time varying stiffness matrix $\boldsymbol{K}_1(t)$ and a damping behavior given by a positive definite matrix $\boldsymbol{D}_1$. The classical compliance controller for the primary task can be designed as

$$\boldsymbol{\tau}_1 = \boldsymbol{J}_1^T \boldsymbol{F}_1 \,, \tag{15}$$

with the control force $\boldsymbol{F}_1$

$$\boldsymbol{F}_1 = -\boldsymbol{K}_1(t)\tilde{\boldsymbol{x}}_1 - \boldsymbol{D}_1 \dot{\boldsymbol{x}}_1 \,, \tag{16}$$

where $\tilde{\boldsymbol{x}}_1 = \boldsymbol{x}_1 - \boldsymbol{x}_{1,d}$ is the task space error. In order to analyze the passivity of this control law, we consider as storage function the associated spring potential

$$S_p = \frac{1}{2}\tilde{\boldsymbol{x}}_1^T \boldsymbol{K}_1(t)\tilde{\boldsymbol{x}}_1 \,. \tag{17}$$

Using (16), the time derivative of S_p becomes

$$\begin{aligned} \dot{S}_p &= \dot{\boldsymbol{x}}_1^T \boldsymbol{K}_1(t)\tilde{\boldsymbol{x}}_1 + \frac{1}{2}\tilde{\boldsymbol{x}}_1^T \dot{\boldsymbol{K}}_1(t)\tilde{\boldsymbol{x}}_1 \\ &= -\dot{\boldsymbol{x}}_1^T \boldsymbol{F}_1 - \dot{\boldsymbol{x}}_1^T \boldsymbol{D}_1 \dot{\boldsymbol{x}}_1 + \frac{1}{2}\tilde{\boldsymbol{x}}_1^T \dot{\boldsymbol{K}}_1(t)\tilde{\boldsymbol{x}}_1 \end{aligned} \tag{18}$$

where passivity with respect to the pair $(-\boldsymbol{F}_1, \dot{\boldsymbol{x}}_1)$ implies passivity with respect to $(-\boldsymbol{\tau}_1, \dot{\boldsymbol{q}})$ since the operator $\boldsymbol{J}$ acts dually in the effort and flow paths. However, passivity of the control law cannot be guaranteed since, although the sign of the dissipated power $\dot{\boldsymbol{x}}_1^T \boldsymbol{D}_1 \dot{\boldsymbol{x}}_1$ is positive semi-definite, the sign of the last term resulting from the stiffness variations is indefinite, and accordingly the primary task controller may be active during periods with increasing stiffness.

Null space controller Similar to the primary task, the goal of the null space controller is to achieve a specific compliance behavior around a virtual equilibrium $\boldsymbol{x}_{2,d}$ with a stiffness $\boldsymbol{K}_2(t)$ and positive definite damping $\boldsymbol{D}_2$. Nevertheless, this goal shall be achieved only as good as possible without disturbing the primary task. We consider the following control law

$$\boldsymbol{\tau}_2 = \boldsymbol{P}\boldsymbol{J}_2^T \boldsymbol{F}_2 \,, \tag{19}$$

with $\boldsymbol{F}_2 = -\boldsymbol{K}_2(t)\tilde{\boldsymbol{x}}_2 - \boldsymbol{D}_2\dot{\boldsymbol{x}}_2$, the task error $\tilde{\boldsymbol{x}}_2 = \boldsymbol{x}_2 - \boldsymbol{x}_{2,d}$ and $\boldsymbol{P} = \boldsymbol{N}(\boldsymbol{q})^T \boldsymbol{Z}(\boldsymbol{q})$ projects into the null space of the primary task. Unfortunately, as explained in Dietrich et al. (2016); Stramigioli (2015), the use of this projection results in a loss of passivity even for a constant stiffness $\boldsymbol{K}_2$, considering that $\boldsymbol{P}$ acts only on force and not dually on velocity. In fact, passivity can be restored if one uses $\dot{\tilde{\boldsymbol{x}}}_2 = \boldsymbol{J}_2 \boldsymbol{P}^T \dot{\boldsymbol{q}}$ and its integration for the implementation of the control law (19). However since $\dot{\boldsymbol{x}}_2$ is given by

$$\begin{aligned} \dot{\boldsymbol{x}}_2 &= \boldsymbol{J}_2 \dot{\boldsymbol{q}} \\ &= \boldsymbol{J}_2(\boldsymbol{J}_1(\boldsymbol{q})^{\boldsymbol{W}+}\dot{\boldsymbol{x}}_1 + \boldsymbol{Z}^T \boldsymbol{v}_n) \,, \end{aligned} \tag{20}$$

recalling that $\boldsymbol{v}_n = \boldsymbol{N}(\boldsymbol{q})\dot{\boldsymbol{q}}$, (20) becomes

$$\dot{\boldsymbol{x}}_2 = \underbrace{\boldsymbol{J}_2 \boldsymbol{J}_1(\boldsymbol{q})^{\boldsymbol{W}+}\dot{\boldsymbol{x}}_1}_{\boldsymbol{\xi}} + \underbrace{\boldsymbol{J}_2 \boldsymbol{P}^T \dot{\boldsymbol{q}}}_{\dot{\tilde{\boldsymbol{x}}}_2} \,, \tag{21}$$

which means that $\dot{\boldsymbol{x}}_2$ features couplings $(\boldsymbol{\xi})$ from the primary task and therefore, using $\dot{\tilde{\boldsymbol{x}}}_2$ instead of $\dot{\boldsymbol{x}}_2$ would not represent anymore the goal of the compliance controller for the null space task. The passivity of the null space control action (19) can be analyzed with the following storage function

$$S_n = \frac{1}{2}\tilde{\boldsymbol{x}}_2^T \boldsymbol{K}_2(t)\tilde{\boldsymbol{x}}_2 \tag{22}$$

which also represents the spring potential energy of the null space controller. Its time derivative is given by

$$\dot{S}_n = \dot{\boldsymbol{x}}_2^T \boldsymbol{K}_2(t)\tilde{\boldsymbol{x}}_2 + \frac{1}{2}\tilde{\boldsymbol{x}}_2^T \dot{\boldsymbol{K}}_2(t)\tilde{\boldsymbol{x}}_2 \tag{23}$$

and using (19), (21)

$$\begin{aligned} \dot{S}_n &= (\boldsymbol{\xi}^T + \dot{\tilde{\boldsymbol{x}}}_2^T)(-\boldsymbol{F}_2 - \boldsymbol{D}_2\dot{\boldsymbol{x}}_2) + \frac{1}{2}\tilde{\boldsymbol{x}}_2^T \dot{\boldsymbol{K}}_2(t)\tilde{\boldsymbol{x}}_2 \\ &= -\dot{\boldsymbol{q}}^T \boldsymbol{\tau}_2 - \dot{\boldsymbol{x}}_2^T \boldsymbol{D}_2 \dot{\boldsymbol{x}}_2 - \boldsymbol{\xi}^T \boldsymbol{F}_2 + \frac{1}{2}\tilde{\boldsymbol{x}}_2^T \dot{\boldsymbol{K}}_2(t)\tilde{\boldsymbol{x}}_2 \end{aligned} \tag{24}$$

where the sign of the last two terms cannot be determined implying that the null space controller is active. Note that, if (19) uses as a state $\bar{\boldsymbol{x}}_2$ instead of $\boldsymbol{x}_2$, the term $\boldsymbol{\xi}^T \boldsymbol{F}_2$ vanishes with $\dot{S}_n$ reducing to

$$\dot{S}_n = -\dot{\boldsymbol{q}}^T \boldsymbol{\tau}_2 - \dot{\tilde{\boldsymbol{x}}}_2^T \boldsymbol{D}_2 \dot{\tilde{\boldsymbol{x}}}_2 + \frac{1}{2}\tilde{\tilde{\boldsymbol{x}}}_2^T \dot{\boldsymbol{K}}_2(t)\tilde{\tilde{\boldsymbol{x}}}_2 \tag{25}$$

with $S_n = \frac{1}{2}\tilde{\tilde{\boldsymbol{x}}}_2^T \boldsymbol{K}_2(t)\tilde{\tilde{\boldsymbol{x}}}_2$ as spring potential and a new error state $\tilde{\tilde{\boldsymbol{x}}}_2 = \bar{\boldsymbol{x}}_2 - \boldsymbol{x}_{2,d}$. (25) means that the controller would be passive with respect to $(-\boldsymbol{\tau}_2, \dot{\boldsymbol{q}})$ for a constant stiffness $(\dot{\boldsymbol{K}}_2(t) = \boldsymbol{0})$.

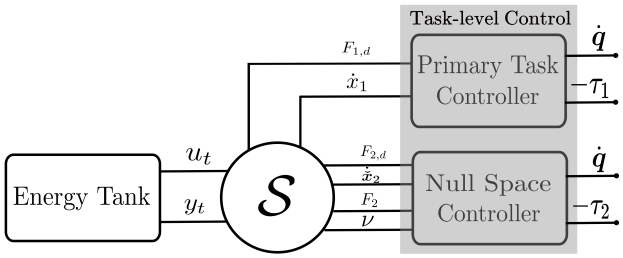

Fig. 2. Interconnection of the energy tank with the primary, null space tasks controllers. The gray block Task level Control corresponds to the same block in Fig. 1

4. CONTROLLERS PASSIFICATION

As shown in the previous section, the primary and null space tasks controllers can become active, and as a result, there exists a passive environment that could destabilize the system when interconnected to the robot (Stramigioli, 2015). Such a consequence is a major safety issue and is certainly not desirable for robots operating close to humans. The loss of passivity in the system can be stated due to the following reasons

- Stiffness variations in the main task controller
- Stiffness variations in the null space task controller
- Projection operator in the null space task controller

The last of these problems was treated in Dietrich et al. (2016). In order to restore passivity in the system, we follow similar lines of thought and employ the concept of *Energy tanks*. We propose a tank design that implements a hybrid impedance-admittance structure, and simultaneously treats the three aforementioned reasons of activity in the system. The central idea behind energy tanks is to allocate a certain energy budget that could be used to execute potentially non-passive control actions. Furthermore, it is possible to harvest the energy dissipated by the system (through the dampers) and re-use it for ensuring passivity.

4.1 Controllers modification

We start by modifying the primary task controller $\boldsymbol{F}_1$ as

$$\boldsymbol{F}_1 = -\boldsymbol{K}_{1,c}\tilde{\boldsymbol{x}}_1 - \boldsymbol{D}_1\dot{\boldsymbol{x}}_1 + \boldsymbol{F}_{1,d}\,, \tag{26}$$

and for the null space controller

$$\boldsymbol{F}_2 = -\boldsymbol{K}_{2,c}\tilde{\check{\boldsymbol{x}}}_2 - \boldsymbol{D}_2\dot{\tilde{\boldsymbol{x}}}_2 + \boldsymbol{F}_{2,d}\,, \tag{27}$$

where $\boldsymbol{K}_1 = \boldsymbol{K}_{1,c} + \boldsymbol{K}_{1,d}(t)$ and $\boldsymbol{K}_2 = \boldsymbol{K}_{2,c} + \boldsymbol{K}_{2,d}(t)$. The terms $\boldsymbol{K}_{1,c}$, $\boldsymbol{K}_{2,c}$ represent the constant stiffness part while $\boldsymbol{K}_{1,d}$, $\boldsymbol{K}_{2,d}$ represent the time varying part. The control actions $\boldsymbol{F}_{1,d}$, $\boldsymbol{F}_{2,d}$ will be used to perform stiffness variations in a passive manner. Furthermore, the new task error is given by $\tilde{\check{\boldsymbol{x}}}_2 = \check{\boldsymbol{x}}_2 - \boldsymbol{x}_{2,d}$ with the new state $\check{\boldsymbol{x}}_2$, which results from integrating

$$\dot{\check{\boldsymbol{x}}}_2 = \boldsymbol{\nu} + \dot{\tilde{\boldsymbol{x}}}_2\,, \tag{28}$$

where the auxiliary control input $\boldsymbol{\nu}$ has the role of preserving the original controller state $\dot{\boldsymbol{x}}_2$ as good as possible while ensuring passivity in the system. The forces $\boldsymbol{F}_{1,d}$, $\boldsymbol{F}_{2,d}$ and $\boldsymbol{\nu}$ will be further derived in the following.

4.2 Energy Tanks

As highlighted earlier, the introduction of the energy tank will be used for restoring passivity in the system. The tank can be viewed as a virtual storage element with arbitrary dynamics interconnected to the controllers in a power preserving manner and will be used to monitor the consequence of non passive control actions. As long as the tank is not empty, the energy left in the tank will be used to "balance" such actions and therefore ensuring passivity. We define a tank with a state $x_t \in \mathbb{R}$, an output variable $y_t \in \mathbb{R}$ and an input variable $u_t \in \mathbb{R}$. The tank dynamics is given by

$$\begin{aligned}\dot{x}_t &= \frac{\beta_1\dot{\boldsymbol{x}}_1^T\boldsymbol{D}_1\dot{\boldsymbol{x}}_1}{x_t} + \frac{\beta_2\dot{\tilde{\boldsymbol{x}}}_2^T\boldsymbol{D}_2\dot{\tilde{\boldsymbol{x}}}_2}{x_t} + u_t \\ y_t &= x_t\end{aligned} \tag{29}$$

The energy stored in the tank is given by

$$S_t = \frac{1}{2}x_t^2 \tag{30}$$

The tank exchanges energy with the controllers through the power port (u_t, y_t). The terms β_1 and β_2 control the amount of energy stored in the tank through dissipation. They are designed as

$$\beta_i = \begin{cases}\kappa_i, & \text{if } S_t < \bar{S}_t\,,\\ 0, & \text{otherwise}\end{cases} \tag{31}$$

for $i = 1, 2$ and with $\kappa_i \in [0, 1]$. The quantity $\bar{S}_t$ is an adequate upper limit for energy stored in the tank. As noted in Lee and Huang (2010), practically unstable control actions could be masked if the energy stored in the tank is not bounded. Note that, if β_1 and β_2 are set permanently to zero, no refilling of the tank is allowed. This means, that as soon as the initial allocated energy budget is consumed, active control actions generating energy could be no longer tolerated.
The tank is interconnected to the controllers through the Dirac structure

$$\begin{bmatrix}\boldsymbol{F}_{1,d}\\ \boldsymbol{F}_{2,d}\\ -\boldsymbol{\nu}\\ u_t\end{bmatrix} = \underbrace{\begin{bmatrix}\boldsymbol{0} & \boldsymbol{0} & \boldsymbol{0} & \boldsymbol{\omega}_1\\ \boldsymbol{0} & \boldsymbol{0} & \boldsymbol{0} & \boldsymbol{\omega}_2\\ \boldsymbol{0} & \boldsymbol{0} & \boldsymbol{0} & \boldsymbol{c}\\ -\boldsymbol{\omega}_1^T & -\boldsymbol{\omega}_2^T & -\boldsymbol{c}^T & \boldsymbol{0}\end{bmatrix}}_{\mathcal{S}}\begin{bmatrix}\dot{\boldsymbol{x}}_1\\ \dot{\tilde{\boldsymbol{x}}}_2\\ \boldsymbol{F}_2\\ y_t\end{bmatrix}, \tag{32}$$

where the matrix $\mathcal{S}$ is skew-symmetric which means that the interconnection is power preserving. As shown in Fig.2, the primary task controller exchanges energy with the Dirac structure through the power port $(\boldsymbol{F}_{1,d}, \dot{\boldsymbol{x}}_1)$, with the energy injected through this power port is used to implement stiffness variations in the primary task. On the other hand, the null space controller is interconnected to the Dirac structure through two power ports: one $(\boldsymbol{F}_{2,d}, \dot{\tilde{\boldsymbol{x}}}_2)$ is used to inject energy necessary for the stiffness variations in the null space task, while the other $(\boldsymbol{F}_2, -\boldsymbol{\nu})$ compensates the null space projection. In terms of causality, the tank acts as a hybrid impedance-admittance.
The design parameters $\boldsymbol{\omega}_1$, $\boldsymbol{\omega}_2$ and $\boldsymbol{c}$ can be regarded as modulating factors that control the power transmission between the tank and the controllers. For $\boldsymbol{\omega}_1$, the choice

$$\boldsymbol{\omega}_1 = -\frac{\sigma(S_t)\boldsymbol{K}_{1,d}(t)\tilde{\boldsymbol{x}}_1}{y_t} \tag{33}$$

is made, with the valve $\sigma(S_t)$ as

$$\sigma(S_t) = \begin{cases}0 < \sigma(S_t) \leq 1 & \text{if } S_t > \underline{S}_t\,,\\ 0 & \text{otherwise}\,,\end{cases} \tag{34}$$

where $\sigma(S_t)$ can be designed to evolve smoothly between 0 and 1 depending on the amount of energy available in the tank. Similarly, the modulating factor $\boldsymbol{\omega}_2$

$$\boldsymbol{\omega}_2 = -\frac{\gamma(S_t)\boldsymbol{K}_{2,d}(t)\tilde{\check{\boldsymbol{x}}}_2}{y_t} \tag{35}$$

where the valve $\gamma(S_t)$ is given by

$$\gamma(S_t) = \begin{cases} 0 < \gamma(S_t) \leq 1 & \text{if } S_t > \underline{S}_t\,, \\ 0 & \text{otherwise}\,. \end{cases} \tag{36}$$

which means that, as long as the tank is not depleted, the controllers can be allowed to perform the time varying stiffness behavior. Note that, in order to avoid singularities, we set a lower limit $\underline{S}_t$ for the energy threshold in the tank. Regarding $\boldsymbol{c}$, it shall be assigned as

$$\boldsymbol{c} = \frac{\alpha(S_t)(\boldsymbol{\xi} + \boldsymbol{\rho}(\boldsymbol{x}_2 - \check{\boldsymbol{x}}_2))}{y_t} \tag{37}$$

where the gain $\boldsymbol{\rho}$ is added to avoid drift as done in Dietrich et al. (2016). As for $\alpha(S_t)$

$$\alpha(S_t) = \begin{cases} 0 < \alpha(S_t) \leq 1 & \text{if } S_t > \underline{S}_t\,, \\ 0 & \text{otherwise}\,. \end{cases} \tag{38}$$

It could be easily confirmed that, as long as energy is available in the tank, the original task coordinate $\boldsymbol{x}_2$ will be used, achieving the original goal of the null space compliance controller. As soon as the energy is empty, compensation for this non-passive control action is no longer supported, and the state $\check{\boldsymbol{x}}_2$ deviates from the original task coordinate $\boldsymbol{x}_2$ retaining passivity in the system, at the expense of some control performance.

5. PASSIVITY PROOF

As shown earlier, the interconnection between the tank and the controllers is power-continuous, i.e no power is lost along the interconnection due to the lossless Dirac structure with the skew symmetry of the matrix $\mathcal{S}$. Therefore, we can analyze the passivity of the sub-system shown in Fig. 2, which consists of the tank and the controllers with the combined storage function

$$S_c = \frac{1}{2}\tilde{\boldsymbol{x}}_1^T\boldsymbol{K}_{1,c}\tilde{\boldsymbol{x}}_1 + \frac{1}{2}\tilde{\check{\boldsymbol{x}}}_2^T\boldsymbol{K}_{2,c}\tilde{\check{\boldsymbol{x}}}_2 + S_t \tag{39}$$

where the new coordinate (28) has been used to define the spring potential of the null space controller. The time derivative of S_c is given by

$$\dot{S}_c = \dot{\boldsymbol{x}}_1^T\boldsymbol{K}_{1,c}\tilde{\boldsymbol{x}}_1 + \dot{\tilde{\check{\boldsymbol{x}}}}_2^T\boldsymbol{K}_{2,c}\tilde{\check{\boldsymbol{x}}}_2 + \dot{x}_t x_t\,. \tag{40}$$

Using (26), (27), (29) and recalling that $\boldsymbol{F}_{1,d} = \boldsymbol{\omega}_1 y_t$, $\boldsymbol{F}_{2,d} = \boldsymbol{\omega}_2 y_t$ from (32), we now have

$$\begin{aligned} \dot{S}_c = &-\dot{\boldsymbol{x}}_1^T\boldsymbol{F}_1 - \dot{\tilde{\check{\boldsymbol{x}}}}_2^T\boldsymbol{F}_2 - \dot{\boldsymbol{x}}_1^T\boldsymbol{D}_1\dot{\boldsymbol{x}}_1 - \dot{\tilde{\check{\boldsymbol{x}}}}_2^T\boldsymbol{D}_2\dot{\tilde{\check{\boldsymbol{x}}}}_2 \\ &+\dot{\boldsymbol{x}}_1^T\boldsymbol{\omega}_1 y_t + \dot{\tilde{\check{\boldsymbol{x}}}}_2^T\boldsymbol{\omega}_2 y_t + \beta_1\dot{\boldsymbol{x}}_1^T\boldsymbol{D}_1\dot{\boldsymbol{x}}_1 + \beta_2\dot{\tilde{\check{\boldsymbol{x}}}}_2^T\boldsymbol{D}_2\dot{\tilde{\check{\boldsymbol{x}}}}_2 \\ &-\boldsymbol{\omega}_1^T\dot{\boldsymbol{x}}_1 x_t - \boldsymbol{\omega}_2^T\dot{\tilde{\check{\boldsymbol{x}}}}_2 x_t - \boldsymbol{c}^T\boldsymbol{F}_2 x_t\,. \end{aligned} \tag{41}$$

Finally, since $y_t = x_t$ and with $\dot{\tilde{\check{\boldsymbol{x}}}}_2 = \boldsymbol{J}_2\boldsymbol{P}^T\dot{\boldsymbol{q}}$ along with (2), (15), (19) and (28), the expression (41) simplifies to

$$\dot{S}_c = -\dot{\boldsymbol{q}}^T(\boldsymbol{\tau}_1 + \boldsymbol{\tau}_2) - (1-\beta_1)\dot{\boldsymbol{x}}_1^T\boldsymbol{D}_1\dot{\boldsymbol{x}}_1 - (1-\beta_2)\dot{\tilde{\check{\boldsymbol{x}}}}_2^T\boldsymbol{D}_2\dot{\tilde{\check{\boldsymbol{x}}}}_2\,. \tag{42}$$

Since the last two terms are negative semi-definite for β_1, β_2 defined according to (31), passivity of the controllers and the energy tank interconnection is guaranteed with respect to the pair $(-(\boldsymbol{\tau}_1 + \boldsymbol{\tau}_2), \dot{\boldsymbol{q}})$.

Intuitively, this can be interpreted as the passification of the parallel interconnection of the primary and the null space tasks controllers. A more conservative solution, however, is to have two local energy tanks interconnected to each controller independently wherein passivity can be shown with respect to $(-\boldsymbol{\tau}_1, \dot{\boldsymbol{q}})$ and $(-\boldsymbol{\tau}_2, \dot{\boldsymbol{q}})$ for the primary and the null space controller, respectively. In this case, energy exchange across levels will no longer occur, and the energy dissipated by one controller will remain on this level.

Now the following statement can be made about the passivity of the overall system:

Proposition 1. Consider the system given by (1) with the closed loop dynamics (12) with $\boldsymbol{\tau}_1$, $\boldsymbol{\tau}_2$ given by (15), (19) and the corresponding control forces $\boldsymbol{F}_1$, $\boldsymbol{F}_2$ defined according to (26), (27) respectively. The controlled robot system defines a passive map with respect to the input $\boldsymbol{\tau}_{ext}$ and the output $\dot{\boldsymbol{q}}$.

The passivity claim follows immediately from the fact that the overall system now is an interconnection of passive subsystems with respect to their corresponding input-output pair, and interconnected through power-conserving Dirac structures. We can consider the following total storage

$$S_o = S_c + S_r \tag{43}$$

which is the sum of kinetic, potential and tank energies in the system. Its rate of change is given by

$$\begin{aligned} \dot{S}_o &= \dot{S}_c + \dot{S}_r \\ &= -\dot{\boldsymbol{q}}^T\boldsymbol{\tau}_c - (1-\beta_1)\dot{\boldsymbol{x}}_1^T\boldsymbol{D}_1\dot{\boldsymbol{x}}_1 - (1-\beta_2)\dot{\tilde{\check{\boldsymbol{x}}}}_2^T\boldsymbol{D}_2\dot{\tilde{\check{\boldsymbol{x}}}}_2 \\ &\quad + \dot{\boldsymbol{q}}^T(\boldsymbol{\tau}_c + \boldsymbol{\tau}_{ext}) \\ &= \dot{\boldsymbol{q}}^T\boldsymbol{\tau}_{ext} - (1-\beta_1)\dot{\boldsymbol{x}}_1^T\boldsymbol{D}_1\dot{\boldsymbol{x}}_1 - (1-\beta_2)\dot{\tilde{\check{\boldsymbol{x}}}}_2^T\boldsymbol{D}_2\dot{\tilde{\check{\boldsymbol{x}}}}_2 \end{aligned} \tag{44}$$

which proves passivity with respect to the port $(\boldsymbol{\tau}_{ext}, \dot{\boldsymbol{q}})$, through which the controlled robot interacts with the environment, which ensures a stable interaction with any passive environment.

6. SIMULATIONS

In order to validate the presented approach, simulations were performed on a 4R-DOF planar manipulator. Each link has 0.5 m length and a 0.5 kg point mass located at the center. The initial configuration is $\boldsymbol{q}_0 = [135°, -90°, -45°, -45°]^\mathsf{T}$. The primary task is an X/Y Cartesian impedance control at the end effector ($\boldsymbol{x}_1 \in \mathbb{R}^2$), while the null space task is a joint level impedance control ($\boldsymbol{x}_2 \in \mathbb{R}^4$). The desired equilibrium configuration of the joint impedance was deliberately chosen not to be feasible given the constraints imposed by the primary task. Therefore, the null space task is in conflict with the primary task and cannot be fully executed, but only as good as possible without disturbing the primary task.

In the first simulation experiment, the compliance behavior for the two tasks was specified with a constant stiffness. Three scenarios were simulated

- Case 1a : Control law without energy tank
- Case 1b : Control law with energy tank, without refilling, i.e. $\beta_{1,2} = 0$
- Case 1c : Control law with energy tank, with refilling and $\beta_{1,2}$ were set to 0.8

In both the second and third scenarios, the tank is initialized with an energy level of 20 J, however in the second

scenario, the dissipated energy by the controllers is completely lost and is not re-used to fill the tank.
The results of this simulation experiment are shown in Fig. 3. Concerning the primary task, it could be observed that the convergence of the error norm $||\tilde{\boldsymbol{x}}_1||$ is identical for all approaches (Fig. 3 (a)), since the primary task controller remains unchanged for all scenarios. On the other hand, the task space error norm of the null space task $||\tilde{\boldsymbol{x}}_2||$ never reaches zero due to the conflict between the primary and the null space task, and therefore only convergence to a constrained local minimum is possible. For Case 1a, the steady state error is lower than the one in Case 1b. This occurs due to the deviation between the new passive coordinate $\check{\boldsymbol{x}}_2$ and the original one $\boldsymbol{x}_2$ shown in Fig. 3 (e), as soon as the tank gets depleted at $t \approx 0.2$, enforcing that the system remains passive at the expense of some control performance. As for Case 1a, the system is clearly not passive as the total energy of the system (Fig. 3 (d)) increases temporarily between $t \approx 0.2$ and $t \approx 0.5$. When re-filling of the tank is allowed (Case 1c), performance is restored and becomes similar to the classical case, as the tank never gets empty.

In the second simulation experiment, we validate the performance for a time varying stiffness profile. For the primary task, the following stiffness profile was specified

$$K_{1,des} = 100 + 10sin(5t) \tag{45}$$

while for the null space task, the desired stiffness profile is $K_{2,des} = 20 + K_{2,d}(t)$ where $K_{2,d}(t)$ is given by

$$K_{2,d}(t) = \begin{cases} 0, & \text{if } t < t_{min}\,, \\ K_f, & \text{if } t > t_{max}, \\ K_f - ((\frac{K_f}{2} + \frac{K_f}{2}cos(\frac{\pi * (t - t_{min})}{(t_{max} - t_{min})})), & \text{otherwise} \end{cases} \tag{46}$$

where the choice $K_f = 5$ was made in this experiment. Three simulation scenarios were tested

- Case 2a : Tank on, without stiffness compensation, i.e σ, γ in (33),(35) are set always to 1
- Case 2b : Tank on with stiffness compensation, without re-filling with σ, γ set according to (34), (36) and $\beta_{1,2} = 0$
- Case 2c : Tank on with stiffness compensation, with re-filling with σ, γ set according to (34), (36) and $\beta_{1,2} = 0.8$

In Case 2a, the controller and the energy tank compensate only for the null space projection operator similar to (Dietrich et al., 2016), without compensating for the time varying stiffness behavior. In all scenarios, the tank was initialized with an energy level of 35 J. The results are shown in Fig. 4. For Case 2a (shown in red), the desired stiffness profile is respected on both levels, however the system loses the safety-critical passivity feature which can be verified in the evolution of the total energy in the system, as energy increases (Fig. 4 (d)). When the tank compensates for stiffness variations, but without re-filling (Case 2b, blue), the time varying stiffness component can be no longer followed as soon as the initial allocated energy budget is consumed, sacrificing performance for the sake of preserving passivity. Nevertheless, routing the dissipated energy back to the tank (Case 2c, black) enhances the performance, while still, ensuring the system remains passive and that energy is monotonically decreasing.

6.1 Discussion

The experimental results shown in the previous section clearly demonstrate that the passivity-based controller formulated ensures passivity. While the differences in performance as compared to the classical controller are not major, the passivity-based controller has the advantage of being passive which means that the controlled robot will always yield stable interactions. Furthermore, the developed controller is energy-aware, in the sense that it is possible to assign context and application dependent energy budgets for the execution of certain non-passive control actions. For example, in situations where the robot interacts with humans, a low energy budget can be chosen such that an unexpected contact between a robot and a human would not lead to injuries. Previous works analyzed the maximum amount of energy a human body can sustain (Newman et al., 2000; Wood, 1971), and an impedance controller that respects such energy and power limitations was developed in Raiola et al. (2018). On the other hand, less conservative energy budgets can be assigned in non-domestic environments where performance would be of higher priority, for instance the accurate reproduction of a time varying stiffness profile during a contact with a surface. In a nutshell, the passivity-based and energy-awareness paradigm for controller design adopted in this work is highly flexible and can serve equally well safety and performance requirements.

7. CONCLUSION

In this work, we presented a passivity-based controller that achieves a time varying impedance behavior for the primary and null space tasks. In order to preserve passivity in the system, the concept of energy tanks is used, which serve as an energy reservoir where an energy budget is allocated for balancing the non-passive control actions, namely, the stiffness variations and the use of the null space projection operator. Furthermore, it is possible to re-route the energy lost in dissipation to increase the tank energy. The approach was validated in simulations, where a time varying stiffness profile was commanded both for the primary and null space tasks. It is shown that, with the introduction of the energy tanks, the system remains passive with the energy always decreasing.
In the future, the approach will be further validated in experiments on a real redundant manipulator, where the robot is required to vary its impedance online during a physical interaction scenario. We will also consider the integration into a whole body controller (Dietrich et al., 2011; Iskandar et al., 2019) for variable impedance tasks.

ACKNOWLEDGEMENTS

This research was funded by the Deutsche Forschungsgemeinschaft (DFG, German Research Foundation) SPP 2134 and the Helmholtz Association.

REFERENCES

Buchli, J., Theodorou, E., Stulp, F., and Schaal, S. (2010). Variable impedance control - a reinforcement learning approach. In *Robotics: Science and Systems*.

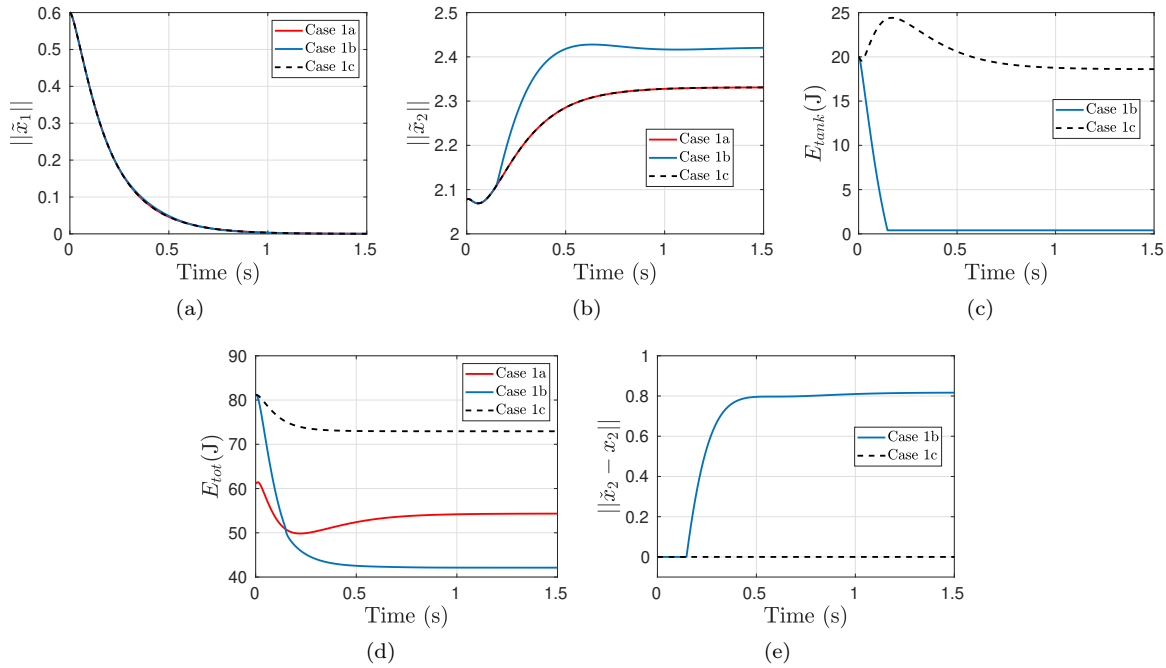

Fig. 3. Experimental results for the constant stiffness case, where the errors on levels one and two, the tank energy, the total energy in the system and the deviation between the original and the new coordinates are shown. Legend: Case 1a: Control law with energy tank deactivated. Case 1b : Tank switched on without refilling. Case 1c: Tank switched on with refilling

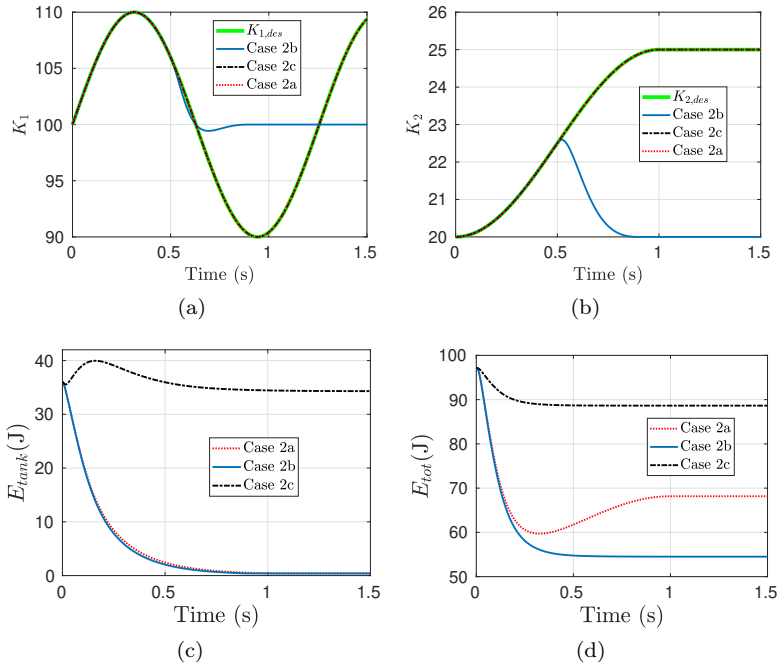

Fig. 4. Results with the time varying stiffness profile. In the upper row, the desired and actual stiffnesses for the primary and null space tasks are shown. In the bottom row, the level of energy in the tank and the total energy in the system are depicted. Legend: Case 2a: Tank switched on without stiffness compensation. Case 2b: Tank switched on with stiffness compensation but without refilling. Case 2c: Tank switched on with stiffness compensation and with refilling.

Dietrich, A., Ott, C., and Stramigioli, S. (2016). Passivation of projection-based null space compliance control via energy tanks. *IEEE Robotics and Automation Letters*, 1(1), pp. 184–191.

Dietrich, A., Wimböck, T., and Albu-Schäffer, A. (2011). Dynamic whole-body mobile manipulation with a torque controlled humanoid robot via impedance control laws. In *2011 IEEE/RSJ International Conference on Intelligent Robots and Systems*, 3199–3206.

Dietrich, A., Wu, X., Bussmann, K., Ott, C., Albu-Schäffer, A., and Stramigioli, S. (2017). Passive hierarchical impedance control via energy tanks. *IEEE Robotics and Automation Letters*, 2(2), 522–529. doi: 10.1109/LRA.2016.2645504.

Duindam, V. and Stramigioli, S. (2004). Port-based asymptotic curve tracking for mechanical systems. *European Journal of Control*, 10(5), 411–420.

Ferraguti, F., Secchi, C., and Fantuzzi, C. (2013). A tank-based approach to impedance control with variable stiffness. In *IEEE International Conference on Robotics and Automation*, 4948–4953.

Ficuciello, F., Villani, L., and Siciliano, B. (2015). Variable impedance control of redundant manipulators for intuitive human–robot physical interaction. *IEEE Transactions on Robotics*, 31(4), 850–863.

Franken, M., Stramigioli, S., Misra, S., Secchi, C., and Macchelli, A. (2011). Bilateral telemanipulation with time delays: A two-layer approach combining passivity and transparency. *IEEE Transactions on Robotics*, 27(4), 741–756.

Franklin, D.W., Osu, R., Burdet, E., Kawato, M., and Milner, T.E. (2003). Adaptation to stable and unstable dynamics achieved by combined impedance control and inverse dynamics model. *Journal of neurophysiology*, 90(5), 3270–82.

Ganesh, G., Jarrassé, N., Haddadin, S., Albu-Schaeffer, A., and Burdet, E. (2012). A versatile biomimetic controller for contact tooling and haptic exploration. In *IEEE International Conference on Robotics and Automation*, 3329–3334.

Hogan, N. (1984). Impedance control: An approach to manipulation. In *American Control Conference*.

Iskandar, M., Quere, G., Hagengruber, A., Dietrich, A., and Vogel, J. (2019). Employing whole-body control in assistive robotics. In *2019 IEEE/RSJ International Conference on Intelligent Robots and Systems (IROS)*, 5643–5650.

Kronander, K. and Billard, A. (2016). Stability considerations for variable impedance control. *IEEE Transactions on Robotics*, 32(5), 1298–1305.

Lee, D. and Huang, K. (2010). Passive-set-position-modulation framework for interactive robotic systems. *IEEE Transactions on Robotics*, 26(2), 354–369.

Lee, D. and Ott, C. (2011). Incremental kinesthetic teaching of motion primitives using the motion refinement tube. *Autonomous Robots*, 31, 115–131.

Liegeois, A. (1977). Automatic supervisory control of the configuration and behavior of multibody mechanisms. *IEEE Trans. on Systems, Man, and Cybernetics*, 7(12), 868–871.

Newman, J.A., Shewchenko, N., and Welbourne, E. (2000). A proposed new biomechanical head injury assessment function - the maximum power index. *Stapp car crash journal*, 44, 215–47.

Ott, C., Artigas, J., and Preusche, C. (2011). Subspace-oriented energy distribution for the time domain passivity approach. In *2011 IEEE/RSJ International Conference on Intelligent Robots and Systems*, 665–671.

Ott, C., Kugi, A., and Yoshihiko Nakamura (2008). Resolving the problem of non-integrability of nullspace velocities for compliance control of redundant manipulators by using semi-definite lyapunov functions. In *IEEE International Conference on Robotics and Automation*, 1999–2004.

Ott, C., Dietrich, A., and Albu-Schäffer, A. (2015). Prioritized multi-task compliance control of redundant manipulators. *Automatica*, 53, 416 – 423.

Park, J., Chung, W., and Youm, Y. (1999). On dynamical decoupling of kinematically redundant manipulators. In *Proceedings IEEE/RSJ International Conference on Intelligent Robots and Systems. Human and Environment Friendly Robots with High Intelligence and Emotional Quotients (Cat. No.99CH36289)*, volume 3, 1495–1500.

Peternel, L., Tsagarakis, N., Caldwell, D., and Ajoudani, A. (2016). Adaptation of robot physical behaviour to human fatigue in human-robot co-manipulation. In *IEEE-RAS International Conference on Humanoid Robots (Humanoids)*, 489–494.

Raiola, G., Cardenas, C.A., Tadele, T.S., de Vries, T., and Stramigioli, S. (2018). Development of a safety- and energy-aware impedance controller for collaborative robots. *IEEE Robotics and Automation Letters*, 3(2), 1237–1244.

Rashad, R., Engelen, J.B.C., and Stramigioli, S. (2019). Energy tank-based wrench/impedance control of a fully-actuated hexarotor: A geometric port-hamiltonian approach. In *International Conference on Robotics and Automation (ICRA)*, 6418–6424.

Schindlbeck, C. and Haddadin, S. (2015). Unified passivity-based cartesian force/impedance control for rigid and flexible joint robots via task-energy tanks. In *2015 IEEE International Conference on Robotics and Automation (ICRA)*, 440–447.

Secchi, C., Stramigioli, S., and Fantuzzi, C. (2007). *Control of Interactive Robotic Interfaces: A Port-Hamiltonian Approach (Springer Tracts in Advanced Robotics)*. Springer-Verlag, Berlin, Heidelberg.

Stramigioli, S. (2015). Energy-aware robotics. In M.K. Camlibel, A.A. Julius, R. Pasumarthy, and J.M. Scherpen (eds.), *Mathematical Control Theory I*, 37–50. Springer International Publishing, Cham.

Tee, K.P., Burdet, E., Chew, C.M., and Milner, T.E. (2004). A model of force and impedance in human arm movements. *Biological Cybernetics*, 90(5), 368–375.

Winter, F., Saveriano, M., and Lee, D. (2016). The role of coupling terms in variable impedance policies learning. In *9th International Workshop on Human-Friendly Robotics (HFR)*.

Wood, J. (1971). Dynamic response of human cranial bone. *Journal of Biomechanics*, 4(1), 1–12.

Yang, C., Ganesh, G., Haddadin, S., Parusel, S., Albu-Schaeffer, A., and Burdet, E. (2011). Human-like adaptation of force and impedance in stable and unstable interactions. *IEEE Transactions on Robotics*, 27(5), 918–930.

Yoshikawa, T. (1985). Manipulability of robotic mechanisms. *The International Journal of Robotics Research*, 4(2), 3–9.